Distributed feedback fiber filter based on apodized fiber Bragg grating

NAZMI A. MOHAMMED, AYMAN W. ELASHMAWY, MOUSTAFA H. ALY[a,*]
Research Center, College of Engineering, Arab Academy for Science, Technology and Maritime Transport, Smart Village, Cairo, Egypt
[a]*Department of Electronics and Communications Engineering, College of Engineering, Arab Academy for Science, Technology and Maritime Transport, Alexandria, Egypt, Member of OSA*

This paper explores the potential of using Distributed Feedback Fiber (DFB-F) under lasing threshold as a C-band optical filter. This is done with the aid of an apodized fiber Bragg grating (FBG) using different apodization profiles. Design optimization is carried out to mainly target Ultra Dense Wavelength Division Multiplexing (UDWDM) filtering specifications. The raised cosine profile DFB-F with grating length (L = 30 mm) and modulation depth ($n_o = 10^{-5}$) is chosen as the most suitable filter for UDWDM filtering specifications. This choice provides a Full Width at Half Maximum (FWHM) of 0.044 nm, no sidelobes and a peak reflectivity of 1.29. Compared to the famous apodized FBG based optical filter, this design gives a remarkable performance combined with compactness and easier fabrication.

1. Introduction

Currently, there is a high level of interest in the fabrication of filters to provide wavelength selectivity and noise filtering in DWDM systems [1]. In these systems, multiplexing/demultiplexing a large number of channels with single wavelength filters would require cascaded filters. The number of filters in a series might be reduced if multichannel band filters are cascaded with a smaller number of single-channel filters [2].

Different filter configurations have been proposed using different optical components such as, optical couplers, Mach-Zehnder lattices, high dispersion fibers, arrayed waveguide gratings (AWGs), or fiber Bragg gratings (FBGs) [3-5]. An FBG acts as an optical filter because of the existence of a stop band, the frequency region in which most of the incident light is reflected back [6].

The spectrum of a good optical filter to be used in DWDM systems must have certain specifications, among them [7-9]; a very narrow bandwidth (BW), weak sidelobe (preferable no side lobe) peaks, i.e., getting high sidelobe suppression ratio (SLSR), ability tune wavelengths in WDM window (0.8-1.6 nm wavelengths spacing), DWDM window (0.2-0.4 nm wavelengths spacing) and UDWDM (wavelength spacing < 0.2 nm).

Apodization represents the variation of the grating modulation strength or coupling coefficient along the grating length to enhance the spectrum performance of the filter [10]. Apodized FBG filters suffer from low selectivity, large sidelobes, and small peak reflectivity making them not suitable for most DWDM/UDWDM

filtering applications [7]. The only mode to overcome previous drawbacks and making apodized FBG filters attractive for DWDM/UDWDM is done by increasing the grating length [11, 12].

Distributed feedback fiber lasers (DFB-FL) have unique features that make them suitable for applications that need single mode operation. They can be designed with a grating structure to provide high output power, single frequency, single polarization, and high optical signal-to-noise ratio [13]. If these characteristics can be accomplished without lasing behavior, it will be really attractive for filtering applications, particularly if more filtering features are added. Apodization with gain under lasing threshold are suggested to be the key parameters to reach the previous idea, the design targets a remarkable active filtering performance suitable for DWDM/UDWDM using a DFB-F. The positive-tanh apodization profile with a grating length (L = 25 mm) and modulation depth ($n_o = 10^{-5}$) provides the most suitable filter for UDWDM filtering specifications with a FWHM of 0.048 nm, suppressed side lobes, and peak reflectivity of 1.906 [14].

The present work extends the study and designs based on [14] by exploring additional apodization functions targeting a better performance optical filter. A parametric study is applied to all apodization functions to optimize the filter performance. Finally, a comparison between the different apodized DFB-F under lasing threshold as an active optical filter is carried out.

This paper is organized as follows: Section 2 presents the proposed structure of the DFB-F and the mathematical model upon which simulation is based. The simulation

results and discussion for various grating lengths and different refractive index variations are reported in Sec.3. This is followed by the main conclusions in Sec.4.

2. Mathematical model

2.1 Coupled mode equations of DFB-Fs

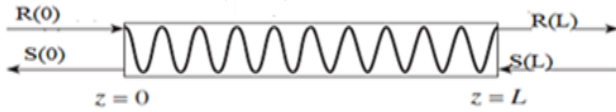The mathematical model used depends on the coupled mode theory as in [14].

Fig. 1. Forward and backward waves in periodic, active waveguides.

Fig. 1 is a schematic of the coupling between forward and backward waves in waveguides induced by periodic modulation of the refractive index n.

For a DFB-F, the coupled-wave equations can be written as [15]

$$\frac{dR(z)}{dz} = (g - j\delta + \frac{1}{2}\frac{d\phi(z)}{dz})R(z) - j\kappa S(z), \quad (1\text{-a})$$

$$\frac{dS(z)}{dz} = -(g - j\delta + \frac{1}{2}\frac{d\phi(z)}{dz})S(z) + j\kappa R(z) \quad (1\text{-b})$$

$$\delta = \beta - \beta_D = 2\pi n_{eff}(\frac{1}{\lambda} - \frac{1}{\lambda_D}) \quad (2)$$

$$\kappa = \frac{\pi}{\lambda} n_o f_A(z) \quad (3)$$

where g is the gain of the DFB active region per unit length, δ is the detuning of the propagation constant from the Bragg condition, n_{eff} is the effective refractive index of the fiber core, λ is the wavelength of the incoming signal, λ_D is the design filter wavelength, κ is the coupling coefficient between the forward and backward waves, L is the grating length, $\phi(z)$ is the wave phase, n_o is the maximum modulation amplitude of refractive index (modulation depth) and $f_A(z)$ is the apodization profile function.

Equation (1) can be merged into a single equation by defining another wave function, then differentiating with respect to z, one can get

$$\frac{du(z)}{dz} + 2(g - j\delta)u(z) - j\kappa(1 + u^2(z)) = 0 \quad (4)$$

where the boundary condition is $u(L) = 0$, representing no backward wave is incident from the other side.

Equation (4) is solved to get the reflection coefficient (r) at the input, i.e., $u(0) = S(0)/R(0)$ and consequently the reflectivity, $|r|^2$. The DFB-F is easily reduced to an FBG when the gain is set to zero [16]. The Rung Kutta 4th order method (RKM4) is used to numerically solve Eq. (4), which has no closed form solution [15].

2.2 Apodization profiles

The main apodization profiles, considered in this investigation, Fig. 2, are [10, 17, and 18]

1)   Raised cosine profile:

$$f_A(z) = \sin^2(\frac{\pi z}{L}) \quad , 0 \le z \le L \quad (5)$$

2)   Blackman profile:

$$f_A(z) = \frac{1 + 1.19\cos(x) + 0.19\cos(2x)}{2.38} \quad ,$$

$$x = \frac{2\pi(z - \frac{L}{2})}{L} \quad , 0 \le z \le L \quad (6)$$

3)   Sigmoid profile:

$$f_A(z) = (1 + 700e^{-1000\left|z - \frac{L}{2}\right|})^{-1} \quad , 0 \le z \le L \quad (7)$$

4)   Bartlett profile:

$$f_A(z) = \begin{cases} \dfrac{2z}{L} & , 0 \le z \le \dfrac{L}{2} \\ -2(\dfrac{z}{L} - 1) & , \dfrac{L}{2} \le z \le L \end{cases} \quad (8)$$

5)   Nuttall profile:

$$f_A(z) = a_0 - a_1\cos(x) + a_2\cos(2x) - a_3\cos(3x) , x = \frac{2\pi z}{L} , 0 \le z \le L \quad (9)$$

$a_o = 0.3635819$,
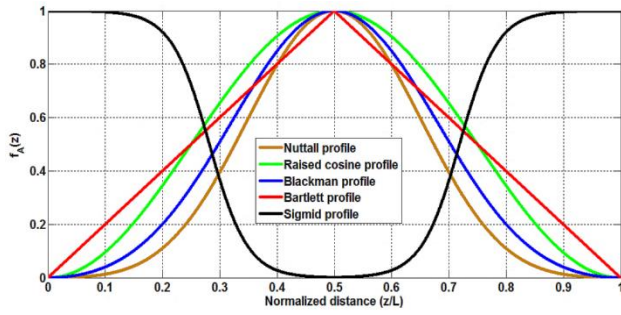$a_1 = 0.4891775$,
$a_2 = 0.1365995$,
and $a_3 = 0.0106411$

Fig. 2. FBG Apodization profiles for DFB-F

Fig. 3. Reflectivity spectrum for a raised cosine
apodization profile at no=10-5

3. Results and discussion

3.1 Introduction

For each apodization profile, the coupling coefficient (κ) is changed according to Eq. (3). The coupling coefficient and Eq. (2) are substituted in Eq. (4) which is then solved numerically using the RKM4 to evaluate the reflectivity. The reflectivity wavelength spectrum is evaluated for different apodization profiles in the DFB-F filter. This is associated with a detailed parametric study for the effect of the grating length (L) and the maximum modulation of the refractive index (n_o). For each apodized DFB-F filter design, optimum values of L and n_o are chosen to produce the best specifications for the optical filter.

The parameters used in simulations are α_s=0.15 m^{-1}, n_{eff} = 1.47 [13]. The grating length varies from 5 mm to 30 mm [17]. The modulation depth, n_o, varies from low (10^{-5}) to large depths (10^{-3}) [18]. The wavelength simulation range is chosen to cover the effective parts of the C-band that are suitable for filtering operations and do not provide a lasing behavior as observed in simulations. The aforementioned parameters provide the ability to compare with other literatures. Finally, the performance of different apodized DFB-F filters is compared followed by a detailed comparison with apodized FBGs.

3.2 Raised cosine apodized DFB-F as an optical filter

Fig. 3 shows the reflectivity wavelength spectrum at different values of L, at constant modulation depth (n_o=10^{-5}). The unclear spectrum observed at (L=5 mm) is presented clearly in insets of Fig. 3.

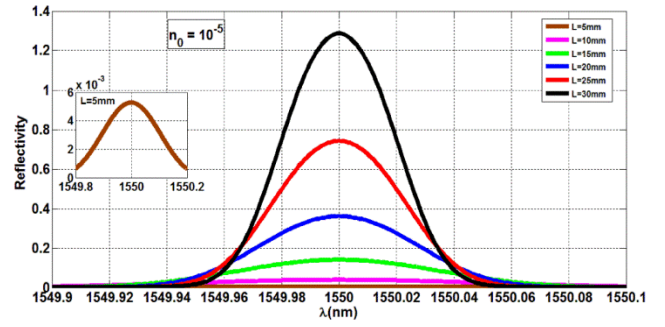As shown, the reflectivity increases and the FWHM decreases with L, and there are no sidelobes. Moreover, for wavelengths near the center designed wavelength λ_D (i.e. $\delta \sim 0$), with sufficiently high gain as in the case of L=30 mm, the condition of oscillation is nearly satisfied and as such the device acts as a high gain amplifier and its reflectivity increases beyond 1.

For optimum filter design, the target is high reflectivity, small FWHM and high SLSR; a compromise between these three parameters should be made. Optimization leads to choosing L=30 mm, providing a peak reflectivity of 1.29 and a FWHM of about 0.044 nm without sidelobes. These parameters can be used for UDWDM filter applications as stated in Sec. 1.

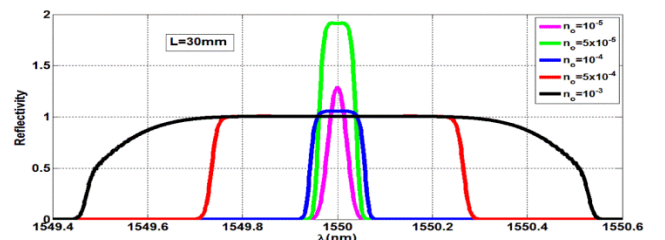Fig. 4 shows the reflectivity wavelength spectrum at different values of n_o, at constant grating length (L = 30 mm).

Fig. 4. Reflectivity of raised cosine apodization profile
at L= 30 mm

It is clear that, the reflectivity increases with n_o then remains at unity for high modulation depths; also the spectrum becomes wider, thus the FWHM increases and no sidelobes exist. Again a compromise must be made while changing n_o and fixing L. The optimum case is n_o=10^{-5} which provides peak reflectivity, smallest FWHM and no sidelobes; like the case of changing L and fixing n_o. Also, the reflectivity increases beyond 1 for the cases of small modulation depths that will nearly achieve the oscillation condition near the center wavelength.

The optimization procedure using the raised cosine apodization was targeting UDWDM filter operation, leading to the previously chosen values for L and n_o.

On the other hand, if less selective filters (only WDM filter applications-wider FWHM) are targeted the modulation depth of the grating can be increased to $n_o=10^{-3}$ which gives a wider FWHM (1.02 nm) and a reflectivity of nearly 1 as shown in Fig. 4. These results can be used as a very good optical band pass filter. This dual filter operation behaviour is available using this apodization profile, the Blackman profile as well as the Bartlett profile as will be provided in Secs. 3.3 and 3.4, respectively.

3.3 DFB-F optical filter using Blackman, Bartlett, Sigmoid and Nuttall apodization profiles

The procedure is repeated for the Blackman, **Bartlett, Sigmoid and Nuttall** apodization profiles resulting in Figs. 5, 6, Figs. 7, 8, Figs. 9, 10, Figs. 11,12 and Figs. 13, 14, respectively
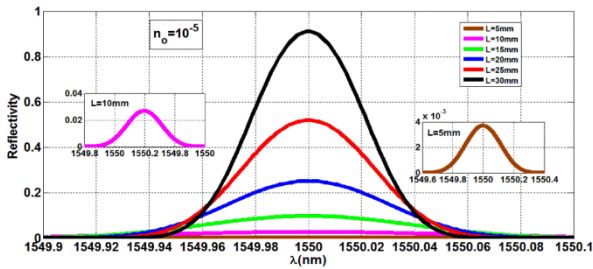

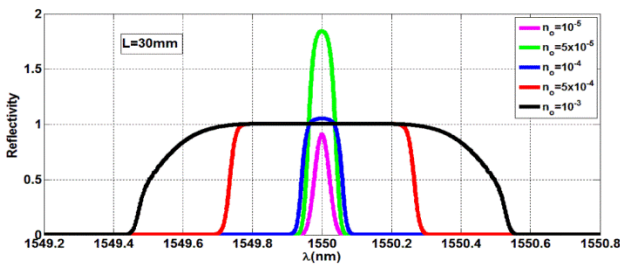Fig. 5. Reflectivity spectrum for Blackman apodization profile at $n_o = 10^{-5}$

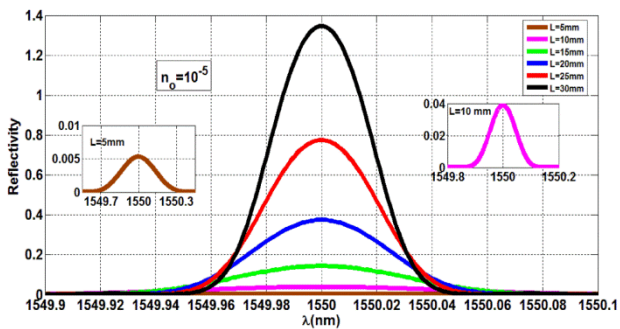Fig. 6. Reflectivity spectrum for Blackman apodization profile at L= 30 mm

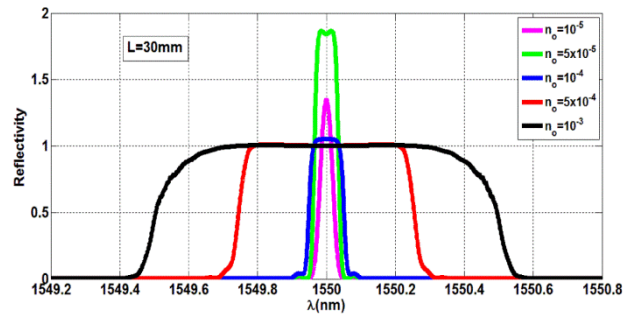Fig. 7. Reflectivity spectrum for the Bartlett apodization profile at $n_o = 10^{-5}$

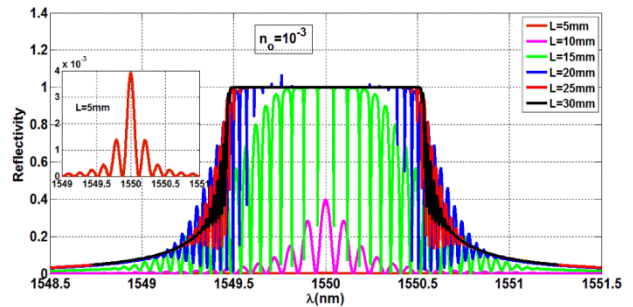Fig. 8. Reflectivity spectrum for the Bartlett apodization profile at L= 30 mm

Fig. 9. Reflectivity of the sigmoid apodization profile at $n_o = 10^{-3}$

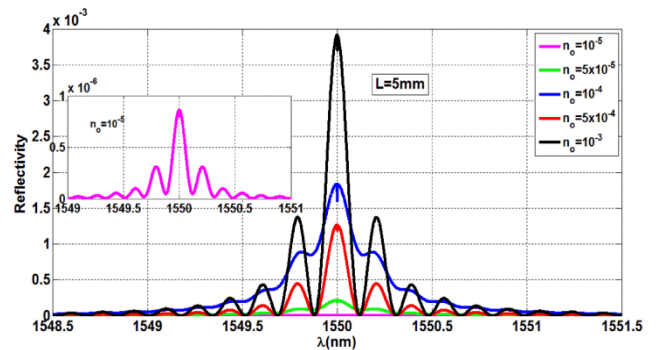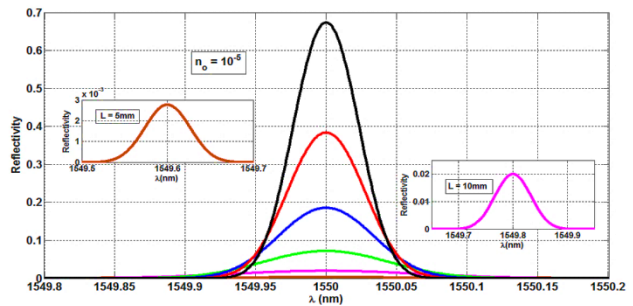Fig. 10. Reflectivity of the sigmoid apodization profile at L = 5 mm

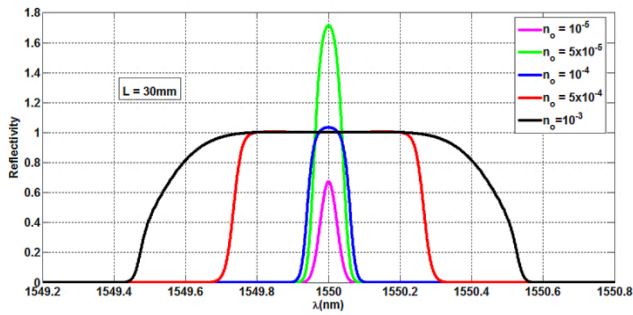Fig. 11. Reflectivity spectrum for the Nuttall apodization profile at $n_o = 10^{-5}$

Fig. 12. Reflectivity spectrum for the Nuttall apodization profile at L = 30 mm

3.4 Comparison

3.4.1 Comparison between apodized DFB-F filter designs

The raised cosine, Bartlett, Blackman, and Nuttall apodization profiles give a smooth response showing no notches in the pass band filter compared to the sigmoid apodization that has a notch at the central wavelength. The notch in the sigmoid profile is about 5.2% as compared to the maximum. This makes the raised cosine, Bartlett, Blackman, and Nuttall profiles better choices when considering only the filter shape response. Table 1 summarizes the observed filtering performance for the different DFB-F apodization profiles.

Table 1. Summary of apodization profiles results

Apodization profile	L (mm)	n_o	FWHM (nm)	Peak Reflectivity	SLSR (dB)	Side lobes	Notch
Raised cosine	30	10^{-5}	0.044	1.29	-	No	No
Blackman	30	10^{-5}	0.05	0.911	-	No	No
Sigmoid	5	10^{-3}	0.116	0.00391	4.55	Yes	5.2%
Bartlett	30	10^{-5}	0.04	1.345	25.7	Yes	No
Nuttall	30	10^{-5}	0.054	0.6741	-	No	No

It is noticed that the best results for raised cosine, Bartlett, Blackman, and Nuttall apodization profiles are achieved at the same long grating length (30 mm) while the Sigmoid profile needs a smaller length. For the Sigmoid profile, a stronger modulation depth is needed to provide reasonable filter performance compared to other profiles. It provides the widest FWHM, smallest SLSR and the smallest reflectivity that result in a degraded filter performance.

The high gain amplification property appears in the raised cosine and Bartlett profiles. For Blackman and Nuttall profiles, although they have the same length and modulation depth, the gain is not as high so the reflectivity is less than 1 and they need larger lengths to achieve the high gain.

The use of Bartlett, raised cosine, Nuttall, and Blackman apodization profiles indicates that they need the same modulation depth (weak coupling) giving very close values of reflectivity and FWHM. Raised cosine, Nuttall, and Blackman profiles have no side lobes while the Bartlett has a small side lobe.

Recall that, concerning specifications that target UDWDM filter applications, an increase in the modulation depth of the raised cosine, Bartlett, Nuttall, and the Blackman apodization profiles leads to a wider reflectivity spectrum curve and an increase in FWHM for the filter, making it suitable for wider WDM filter applications.

3.4.2 Comparison with related work

Table 2 shows the features of some famous profiles for apodized FBGs that are used as filters [7, 11, 12, 16, 20-24].

As shown in Tables 1 and 2, the DFB-F raised cosine profile needs less modulation depth compared to the FBG raised cosine profile of the same length (30 mm), giving a narrower FWHM and higher reflectivity that makes it better for more selective filters.

For the Blackman profile, the DFB-F needs a shorter grating length to get nearly the same narrow FWHM (0.05 nm) and equal reflectivity (0.91) resulting in a more compact size and better design which is easier to fabricate due to the weak modulation depth.

Concerning the DFB-F Bartlett profile, the weak modulation depth and small grating length that give a much narrower FWHM and higher reflectivity make it better than most of the apodized FBGs in Table 2. However, it results in a SLSR of 25.7 dB due to the existence of sidelobes which is a disadvantage as compared to other profiles.

Table 2. Comparison with related work

Apodization Profile	L (mm)	n_o	FWHM (nm)	Peak Reflectivity	SLSR (dB)	Side lobes	Reference no.
Uniform	10	10^{-4}	0.15	0.92	8	Yes	20
Raised cosine	30	10^{-5}	0.044	1.29	-	No	Present Work
Raised cosine	30	2×10^{-4}	0.18	1	-	No	20
Raised cosine	45	10^{-4}	0.1	0.999	-	No	12
Blackman	30	10^{-5}	0.05	0.911	-	No	Present Work
Blackman	100	10^{-3}	0.04	0.92	-	No	21
Sigmoid	5	10^{-3}	0.116	0.00391	4.55	Yes	Present Work
Bartlett	30	10^{-5}	0.04	1.345	25.7	Yes	Present Work
Nuttall	30	10^{-5}	0.054	0.6741	-	No	Present Work
Gaussian	10	2×10^{-4}	0.16	0.915	18	Yes	7
Inverse Gaussian	8	4×10^{-4}	0.2	0.9958	4.5	Yes	23
Tanh	100	0.77	0.06	1	1.5	Yes	11
Positive tanh	100	10^{-5}	0.2	0.999	-	No	16
Hamming	100	0.77	0.02	0.75	9	Yes	11
Cauchy	100	0.77	0.03	1	2.6	Yes	11
Triangular spectrum FBG	100	2.27×10^{-4}	6	0.8	-	No	22
Triangular FBG with asymmetrical spectrum	2	5×10^{-4}	1	1	-	No	24

The DFB-F Sigmoid profile gives a narrower FWHM (0.116 nm) and a higher SLSR compared to some of the tabulated FBGs, but the existence of a notch in its central wavelength and the very small reflectivity (0.00391) makes it a better choice.

The DFB-F Nuttall profile gives a narrower FWHM (0.054 nm) and a better sidelobe suppression, resulting in a more selective filter, irrespective of its small reflectivity (0.6741).

Generally, this work shows that careful choice of the apodized DFB-F that provides active optical filters with weaker modulation depths, higher reflectivity, higher SLSRs and narrower FWHM.

4. Conclusion

This work explores the viability of using apodized DFB-Fs as accurate C-band optical filters. It proves the effect of the apodization profile on the filter performance.

For UDWDM filter applications, no apodization profile fulfils all perfect optical filter requirements. Although the raised cosine seems the best profile, a trade-off should be carried out by carefully selecting a suitable grating length and modulation depth to achieve the best performance according to UDWDM system filtering requirements.

References

[1] Ting-Ting Song Yong Zhao, Zhu-Wei Huo, J. Lightwave Technol., **29**, 3672 (2011).

[2] Radan Slavík, Sophie La Rochelle, IEEE Photon. Technol. Lett., **14**, 1704 (2002).

[3] S. Iezekiel T. A. Cusick, R. E. Miles, S. Sales, J. Capmany, IEEE Trans. Microwave Theory and Tech., **45**, 1458 (1997).

[4] S. Johns D. Norton, C. Keefer, R. Soref, IEEE Photon. Technol. Lett., **6**, 831 (1994).

[5] B. Vidal V. Polo, J. L. Corral, J. Marti, Novel IEEE Photon. Technol. Lett., **15**, 584 (2003).

[6] R. Kashyap, Fiber Bragg Gratings, Academic Press, San Diego, CA, 1999.

[7] Monia Najjar Moez Ferchichi, Houria Rezig, Proceeding of the IEEE International Conference on Transparent Optical Networks "Mediterranean Winter", Marrakech, Morocco, pp. 1-5, 2008.

[8] ITU-T, Transmission Media and Optical Systems Characteristics –Characteristics of Optical Systems, in Spectral Grids for WDM Applications: DWDM Frequency Grid, (Switzerland-Geneva: International Telecommunication Union, pp. G.680-G.699, 2012.

[9] Monia Najjar Moez Ferchichi, Houria Rezig, Proceeding of the 17th IEEE International Conference on Telecommunications (ICT), Doha, Qatar, 538 (2010).

[10] Nazmi A. Mohammed, Taha A. Ali, Moustafa H. Aly, Optics and Lasers in Engineering, **55**, 22 (2014).

[11] Sher Shermin A. Khan, Md. S. Islam, J. Communications, **7**, 840 (2012).

[12] Rachida Hedara Abdallah Ikhlef and Mohamed Chikh-bled, International J. Computer Science, **9**, 368 (2012).

[13] P. Varming, M. Kristensen J. Hübner, Electron. Lett., **33**, 139 (1997).

[14] Nazmi A. Mohammed, Ayman W. Elashmawy, and Moustafa H. Aly, Journal of Modern Optics, **60**, 1701 (2013).

[15] Andy L. Y. Low Kian Yong Lim, Su Fong Chien, H. Ghafouri-Shiraz, IEEE J. Selected Topics in Quantum Electron., **11**, 913 (2005).

[16] Mikhail N. Zervas Karin Ennser, Richard I. Laming, IEEE J. Quantum Electron., **34**, 770 (1998).

[17] D. Sen A. I. Azmi, G. D. Peng, Proceeding of Photonics North **7386**, Quebec, Canada, pp. 73860K1-73860K11, 2009.

[18] Taymour A. Hamdallah Osama Mahran, Moustafa H. Aly, Ahmed E. El-Samahy, J. Applied Sciences Research, **5**, 1604 (2009).

[19] D. Gonze, Daniel T. Gillespie, Numerical Methods to Solve Ordinary Differential Equations, 2009, http://homepages.ulb.ac.be/~dgonze/TEACHING/numeric s.pdf (accessed Sep 2, 2013).

[20] Turan Erdogan, J. Lightwave Technol., **15**, 1277 (1997).

[21] K. Tamura T. Komukai, M. Nakazawa, IEEE Photon. Technol. Lett., **9**, 934 (1997).

[22] Dejun Feng Mingshuang Lv, Dongzhou Yang, Proceeding of The Pacific Rim Conference on Lasers and Electro-Optics (CLEO / PACIFIC RIM '09), Shanghai, pp. 1-2, 2009.

[23] Maarg Nguse Welehtsan, B. B. Padhy, J. Emerging Trends in Engineering and Applied Sciences, **2**, 921 (2011).

[24] Chao-Kai Wen Jung-Chieh Chen, Pangan Ting, IEEE Photon. Technol. Lett., **25**, 295 (2013).

_____

[*]Corresponding author: drmosaly@gmail.com